Genetic interactions between the DBL-1/BMP-like pathway and *dpy* body size–associated genes in *Caenorhabditis elegans*

Mohammed Farhan Lakdawala[a], Bhoomi Madhu[a], Lionel Faure[a], Mehul Vora[b], Richard W. Padgett[b,c,d], and Tina L. Gumienny[a,*]

[a]Department of Biology, Texas Woman's University, Denton, TX 76204-5799; [b]Waksman Institute of Microbiology, [c]Waksman Institute of Microbiology Department of Molecular Biology and Biochemistry, and [d]Cancer Institute of New Jersey, Rutgers University, Piscataway, NJ 08854-8020

ABSTRACT **Bone morphogenetic protein (BMP) signaling pathways control many developmental and homeostatic processes, including cell size and extracellular matrix remodeling. An understanding of how this pathway itself is controlled remains incomplete. To identify novel regulators of BMP signaling, we performed a forward genetic screen in *Caenorhabditis elegans* for genes involved in body size regulation, a trait under the control of BMP member DBL-1. We isolated mutations that suppress the long phenotype of *lon-2*, a gene that encodes a negative regulator that sequesters DBL-1. This screen was effective because we isolated alleles of several core components of the DBL-1 pathway, demonstrating the efficacy of the screen. We found additional alleles of previously identified but uncloned body size genes. Our screen also identified widespread involvement of extracellular matrix proteins in DBL-1 regulation of body size. We characterized interactions between the DBL-1 pathway and extracellular matrix and other genes that affect body morphology. We discovered that loss of some of these genes affects the DBL-1 pathway, and we provide evidence that DBL-1 signaling affects many molecular and cellular processes associated with body size. We propose a model in which multiple body size factors are controlled by signaling through the DBL-1 pathway and by DBL-1–independent processes.**

Monitoring Editor
Jeffrey D. Hardin
University of Wisconsin

Received: Sep 9, 2019
Revised: Oct 22, 2019
Accepted: Nov 1, 2019

INTRODUCTION

The bone morphogenetic protein (BMP) family of signaling ligands, a group within the transforming growth factor-β (TGF-β) superfamily, are used by animal cells to convey developmental and homeostatic messages. Target cells receive the secreted BMP ligands and convert the cues into cell-specific transcriptional responses. How BMP pathways control and are controlled by cells is complex and incompletely clarified. In the roundworm *Caenorhabditis elegans*, the BMP member DBL-1 has a well-defined pathway that includes the core components and conserved regulators, such as the negative regulator LON-2/glypican. There are clear, dose-dependent phenotypes associated with this pathway, including body size. Loss of DBL-1 signaling leads to small body size, while increased signaling results in long animals (Brenner, 1974; Savage *et al.*, 1996; Krishna *et al.*, 1999; Morita *et al.*, 1999). Genetic screens and powerful molecular techniques available in *C. elegans* have been used to isolate, identify, and characterize DBL-1 and associated conserved BMP pathway players (Brenner, 1974; Savage *et al.*, 1996; Krishna *et al.*, 1999; Suzuki *et al.*, 1999; Savage-Dunn *et al.*, 2003; Gumienny *et al.*, 2007, 2010; Liang *et al.*, 2007; Gleason *et al.*, 2017).

Previous screens for body size mutants have been done by mutagenizing otherwise wild-type animals. To increase the likelihood of identifying new modulators of the pathway, we performed a forward genetic screen using a sensitized background, *lon-2(e678)*. Because this genotype increases DBL-1 pathway signaling and causes a long-body phenotype, we expected that we could isolate alleles that cause mild changes in body length that may not have been identified

This article was published online ahead of print in MBoC in Press (http://www.molbiolcell.org/cgi/doi/10.1091/mbc.E19-09-0500) on November 6, 2019.

*Address correspondence to: Tina L. Gumienny (tgumienny@twu.edu).

Abbreviations used: ADAMTS, a disintegrin and metalloproteinase domain with thrombospondin motif; BMP, bone morphogenetic protein; ECM, extracellular matrix; EMS, ethyl methanesulfonate; GFP, green fluorescent protein; GPI, glycosylphosphatidylinositol; IFT, intraflagellar transport; IPTG, isopropyl β-D-1-thiogalactopyranoside; RNAi, RNA interference; TGF-β, transforming growth factor-β.

Gene	Known allele	Function or homology (*Drosophila*)	Allele isolated
A. Alleles of DBL-1 pathway genes			
dbl-1	*wk70*	TGF-β-like ligand	*wk91*, *wk92*
sma-6	*e1482*	Type I receptor	*wk87*, *wk103*, *wk129*, *wk134*
sma-2	*e502*	Smad	*wk83*, *wk84*
sma-3	*e491*	Smad	*wk107*
sma-4	*e729*	Smad	*wk85*
sma-9	*wk55*	Transcription regulator (Schnurri)	*wk97*, *wk131*
sma-10	*wk66*	LRIG (binds receptors to facilitate signaling)	*wk88*, *wk89*, *wk90*
kin-29/sma-11	*wk26*	Kinase	*wk117*
B. Alleles of uncloned *sma* genes			
sma-12	*wk69*	Positive body size effector	*wk119*
sma-13	*wk52*	Positive body size effector	*wk109*
—	-	Positive body size effector	*wk94*
—	-	Positive body size effector	*wk98*
—	-	Positive body size effector	*wk123*
C. Alleles of ECM-associated genes			
dpy-1	*e1*	Mucin-like	*wk111*, *wk142*, *wk143*
dpy-2	*e8*	Collagen (Viking)	*wk104*, *wk122*
dpy-3	*e27*	Collagen (Col4a1)	*wk105*
dpy-4	*e1166*	Collagen (Col4a1)	*wk101*, *wk102*
dpy-5	*e61*	Collagen (Col4a1)	*wk137*
dpy-6	*e14*	Mucin-like	*wk113*, *wk118*, *wk127*, *wk132*
dpy-7	*e88*	SFTPD (collagen-containing C-type lectin) (Col4a1)	*wk106*
dpy-8	*e130*	Collagen (Viking)	*wk120*
dpy-9	*e12*	Collagen (Col4a1)	*wk124*
dpy-13	*e184*	Collagen (Viking)	*wk95*, *wk135*, *wk145*
dpy-14	*e188*	Collagen (Viking)	*wk116*, *wk128*
dpy-17	*e164*	Collagen (Viking)	*wk140*
D. Alleles of other body size-associated genes			
dyf-11	*wk57*	Intraflagellar transport particle B component (IFT54)	*wk136*, *wk139*
dpy-20	*e1282*	BED zinc finger protein	*wk141*

TABLE 1: Alleles isolated in an EMS screen that suppress the *lon-2(e678)* long body size.

in the wild-type background used in previous screens (Brenner, 1974; Savage-Dunn *et al.*, 2003). Suppressors were expected either to act downstream of LON-2 in the DBL-1 signaling pathway or to render animals smaller or shorter independent of DBL-1 signaling. In this screen, we identified additional genetic interactions between the BMP-like DBL-1 pathway and cellular processes and components affecting body size. Here, we analyze genetic interactions between the DBL-1 pathway and other processes that affect body size.

RESULTS AND DISCUSSION

Isolation of alleles of known DBL-1 pathway signaling components

LON-2 is a conserved glypican, a heparan sulfate proteoglycan that inhibits DBL-1 from activating its receptors (Gumienny *et al.*, 2007). Loss of LON-2 results in increased DBL-1 pathway signaling and a long-body phenotype (Brenner, 1974). We performed an EMS mutagenesis F2 screen for animals with recessive mutations that reduce the body length of *lon-2(e678)* animals. We isolated and characterized 46 alleles from a screen of ~9000 mutagenized genomes, which is less than saturation (Table 1). As expected, multiple alleles of core DBL-1 signaling pathway components were isolated (Table 1A). Two alleles of the *dbl-1* gene encoding the ligand, *wk91* and *wk92*, were confirmed by complementation testing with *dbl-1(wk70)*. Four alleles of the gene encoding the *sma-6* Type I receptor, *wk87*, *wk103*, *wk129*, and *wk134*, were confirmed by genetic testing with *sma-6(e1482)*. Two alleles of the R-Smad *sma-2* gene, *wk83* and *wk84*, were identified by noncomplementation with *sma-2(e502)*. The co-Smads *sma-3* and *sma-4* are represented in

this screen by *sma-3(wk107)* and *sma-4(wk85)*, confirmed by complementation testing with *sma-3(e491)* and *sma-4(e729)*, respectively. Two alleles of the Smad regulator Schnurri homologue *sma-9*, *wk97* and *wk131*, were shown to be allelic to *sma-9(wk55)*. Three alleles were isolated for *sma-10*, a pathway regulator that interacts physically with the DBL-1 receptor complex and promotes DBL-1 pathway signaling. *wk88, wk89,* and *wk90* did not complement *sma-10(wk66)* (Gumienny *et al.,* 2010). *sma-11/kin-29* is a serine–threonine kinase gene that acts genetically between *dbl-1* and *lon-1*, a DBL-1 pathway target gene (Maduzia *et al.,* 2005). *wk117* fails to complement *kin-29(wk26)*. Because we selected against alleles that were dauer constitutive, we did not isolate *daf-4* Type I receptor mutations. These results show that this screening approach was successful for isolating DBL-1 pathway–associated alleles.

Isolation and mapping of alleles of unknown loci

This screen also provided additional alleles of uncloned genes (Table 1B). *wk119* is allelic to *sma-12(wk69)* V, and *wk109* is allelic to *sma-13(wk52)* I (Savage-Dunn *et al.,* 2003). Three loci remain unnamed. Another allele, *wk94,* was mapped to chromosome II and complements *sma-6*, *dpy-2*, and *dpy-10*. It is slow-growing. *wk123* also maps to Chromosome II and complements *sma-6*, *dpy-2*, *dpy-10*, and *wk94*. *wk98* maps to Chromosome III and is not allelic to *daf-4*, *sma-2*, *sma-3*, *sma-4*, or *sma-17(wk59)*. *wk98* males have a normal male tail and mate well, unlike most alleles of DBL-1 core-pathway genes.

Isolation of alleles of extracellular matrix–associated genes

Many gene products contribute to the *C. elegans* cuticle, a specialized extracellular matrix (ECM) that protects animals. Loss of some cuticle-associated genes produces a reduced body size (Page and Johnstone, 2007). Alleles of several collagen genes were isolated in the *lon-2* suppressor screen (Table 1C). These loci were identified by their failure to complement published *dpy* alleles (see Table 1 for alleles tested). *wk116* and *wk128* are alleles of collagen type III alpha 1-like gene *dpy-14*. Alleles of genes encoding proteins with collagen domains were isolated: *dpy-2* (*wk104* and *wk122*), *dpy-3/dpy-12 (wk105)*, *dpy-4* (*wk101* and *wk102*), *dpy-5* (*wk137*), *dpy-7* (*wk106*), *dpy-8* (*wk120*), *dpy-9/col-100* (*wk124*), *dpy-13* (*wk95*, *wk135*, and *wk145*), and *dpy-17* (*wk140*).

The screen also produced alleles of two mucin-like genes, *dpy-1* (*wk111*, *wk142*, and *wk142*) and *dpy-6* (*wk113*, *wk118*, *wk127*, and *wk132*; Table 1C; S. Eimer, personal communication, July 18, 2019; Shen *et al.,* 2008). Mucins are glycosylphosphatidylinositol (GPI)-anchored cell surface glycoproteins that are components of the *C. elegans* cuticle's surface coat. In other systems, mucins are transcriptionally regulated by the TGF-β pathway (Jonckheere *et al.,* 2004a,b). Human mucin 1 is required for TGF-β expression, secretion, and activity (Li *et al.,* 2015a,b; Grover *et al.,* 2018).

Isolation of alleles of other body size–associated genes

Loss of some intraflagellar transport (IFT) components is associated with a reduced body size (Starich *et al.,* 1995; Kobayashi *et al.,* 2007). We discovered that *wk136* and *wk139* are allelic to *dyf-11(mn392)*, which produces "slightly short" animals and affects a protein related to TRAF3IP1 (TRAF3 interacting protein 1)/MIP-T3 (microtubule-interacting protein that interacts with TRAF3, the tumor necrosis factor receptor–associated factor 3). MIP-T3 is associated with intraflagellar transport particle B, a complex that transports cargo to the tip of flagella and cilia (Starich *et al.,* 1995; Bacaj *et al.,* 2008). *wk139* and *wk136* are also allelic to previously uncloned *sma-16(wk57)*, which has a similar mild small body size phenotype (Table 1D; Savage-Dunn *et al.,* 2003). This result suggests that the small body size associated with loss of IFT suppresses DBL-1 pathway-mediated body size. Future work will determine whether the mechanism of this body size suppression is independent of DBL-1 signaling.

dpy-20 encodes a novel BED zinc-finger protein required for normal body morphology, movement, male mating (but not ray morphology), and germ cell proliferation (Hodgkin, 1983; Baird and Emmons, 1990; Clark *et al.,* 1995; Schertel and Conradt, 2007; Yemini *et al.,* 2013). A role as a transcription regulator, a common (but not exclusive) role for other BED zinc-finger-containing proteins, has been suggested for DPY-20 (Aravind, 2000). Transcriptional regulation of cuticle genes by DPY-20 is supported by observed changes in cuticle structure in animals with absent or reduced levels of DPY-20 (Clark *et al.,* 1995). An allele of *dpy-20*, *wk141*, was isolated in the *lon-2* suppressor screen (Table 1D). In addition to the dumpy body shape, *wk141* animals also displayed a round head characteristic of *dpy-20* (unpublished data; Clark *et al.,* 1995).

Loss of *dpy* gene function reduces body size of animals overexpressing DBL-1

LON-2 is a glypican that normally sequesters DBL-1 ligand and prevents DBL-1 from activating receptors that mediate body size gene expression (Gumienny *et al.,* 2007). Loss of LON-2 results in long animals (Brenner, 1974). Overexpressing DBL-1 also results in long animals (Morita *et al.,* 1999; Schultz *et al.,* 2014). To generate a more comprehensive understanding of the interaction of DBL-1 signaling with other factors that have strong effects on body size, we asked whether loss of the function of a panel of genes affecting body size in *C. elegans* can suppress the long body size defect exhibited by animals overexpressing DBL-1. This panel includes all *dpy* genes identified in the screen and *dpy-10*, *dpy-11*, *sqt-3/dpy-15*, *dpy-18*, *dpy-19*, *dpy-21*, *dpy-23*, and *blmp-1/dpy-24*, for which alleles were not isolated. Regardless of gene function, most *dpy(RNAi)*s and all *dpy* mutants tested in green fluorescent protein (GFP)-tagged DBL-1 overexpressing backgrounds are significantly shorter than the controls (Supplemental Table S2). Thus, all *dpy* mutants tested suppress the long phenotype associated with overexpressed GFP-tagged DBL-1.

Some extracellular matrix–associated genes interact genetically with the DBL-1 pathway

In *C. elegans*, signaling by the DBL-1 pathway controls components that form the cuticle, a specialized ECM that not only provides a barrier between the animal and its environment, but also affects the size of the organism within it (Mochii *et al.,* 1999; Liang *et al.,* 2007; Luo *et al.,* 2009; Roberts *et al.,* 2010; Madaan *et al.,* 2018). Possibly because the *C. elegans* cuticle is dynamic, with different constituents composing the cuticle of each of its developmental stages, different cuticle component genes were identified in these studies. Altering the cuticle content by reduced DBL-1 signaling may underlie *dbl-1* loss-of-function phenotypes besides smaller body length, including male tail ray fusions, increased cuticular permeability, and "worm-star" formation by clusters of nematodes becoming entangled by their tails (Savage *et al.,* 1996; Morita *et al.,* 1999; Suzuki *et al.,* 1999; Schultz *et al.,* 2014). However, loss of single cuticular proteins can also alter nematode body length, possibly independent of the DBL-1 pathway (Brenner, 1974; Nystrom *et al.,* 2002; Page and Johnstone, 2007; Fernando *et al.,* 2011).

We tested for interaction of selected genes with the DBL-1 pathway in two ways. First, we used a functional GFP-tagged DBL-1 (GFP::DBL-1) translational reporter (*dbl-1p::gfp::dbl-1*) to determine

Gene	Genotype	*dbl-1::gfp* fluorescence % control ± 95% CI	*p* value	Genotype	*spp-9p*::GFP fluorescence % control ± 95% CI	*p* value
A. Controls						
Control	*texIs100*	100 ± 15.57		*texIs127*	100 ± 11.47	
Control	*texIs101*	100 ± 25.95		*wkIs40*	100 ± 13.20	
B. ECM-associated genes						
dpy-1	*dpy-1(e1); texIs100*	96.02 ± 40.89	0.8335	*dpy-1(e1); texIs127*	100.80 ± 16.97	0.9234
dpy-2	*dpy-2(e8); texIs100*	115 ± 52.15	0.5080	*dpy-2(e8); texIs127*	107.04 ± 12.20	0.2344
dpy-3	*texIs100; dpy-3(e27)*	43.45 ± 21.63	0.0012	*wkIs40; dpy-3(e27)*	156.26 ± 16.06	0.0001
dpy-4	*dpy-4(e1166); texIs101*	102.24 ± 28.06	0.9043	*dpy-4(e1166); texIs127*	125 ± 25.16	0.0192
dpy-5	*dpy-5(e61); texIs100*	54.13 ± 26.47	0.0127	*dpy-5(e61); texIs127*	155.23 ± 25.16	0.0001
dpy-6	*texIs101; dpy-6(e14)*	59.96 ± 17.12	0.0009	*wkIs40; dpy-6(e14)*	179.04 ± 19.77	0.0001
dpy-7	*texIs100; dpy-7(e88)*	79.88 ± 34.85	0.2689	*wkIs40; dpy-7(e88)*	104.89 ± 12.95	0.4299
dpy-8	*texIs100; dpy-8(e130)*	79.64 ± 26.74	0.1828	*wkIs40; dpy-8(e130)*	92.68 ± 11.12	0.2061
dpy-9	*dpy-9(e12); texIs101*	95.02 ± 29.01	0.7248	*dpy-9(e12); texIs127*	100.29 ± 10.24	0.9533
dpy-10	*dpy-10(e128); texIs100*	61.46 ± 2 4.99	0.0172	*dpy-10(e128); texIs127*	115.50 ± 11.56	0.0054
dpy-11	*texIs100; dpy-11(e224)*	92.10 ± 28.95	0.6094	*dpy-11(e224); texIs127*	128.88 ± 18.06	0.0007
dpy-13	*dpy-13(e184); texIs101*	91.98 ± 30.42	0.5829	*dpy-13(e184); texIs127*	156.65 ± 24.39	0.0001
dpy-14	*dpy-14(e188); texIs100*	64.97 ± 2 6.13	0.0289	*dpy-14(e188); texIs127*	142.81 ± 22.04	0.0001
dpy-15	*texIs100; dpy-15(e24)*	99.14 ± 43.40	0.9654	*dpy-15(e24); texIs127*	86.33 ± 19.32	0.1875
dpy-17	*dpy-17(e164); texIs100*	80.99 ± 29.16	0.1969	*dpy-17(e164); texIs127*	121.07 ± 17.84	0.0116
dpy-18	*dpy-18(e364); texIs100*	96.43 ± 36.45	0.8543	*dpy-18(e364); texIs127*	110.60 ± 15.13	0.1336
C. Other body size–associated genes						
dpy-19	*dpy-19(e1259); texIs100*	109.22 ± 47.09	0.6514	*dpy-19(e1259); texIs127*	132.90 ± 29.35	0.0107
dpy-20	*dpy-20(e1282); texIs101*	91.56 ± 54.19	0.7181	*dpy-20(e1282); texIs127*	109.77 ± 15.57	0.1818
dpy-21	*texIs100; dpy-21(e428)*	110.37 ± 44.89	0.6011	*dpy-21(e428); texIs127*	116.86 ± 11.93	0.0033
dpy-23	*texIs100;dpy-23(e840)*	39.87 ± 14.82	0.0005	*wkIs40;dpy-23(e840)*	120.47 ± 13.55	0.0015
dpy-24	*dpy-24(s71); texIs100*	59.89 ± 22.45	0.0182	*dpy-24(s71); texIs127*	135.42 ± 19.64	0.0001

TABLE 2: Effects of body size–associated genes on GFP::DBL-1 and DBL-1 pathway reporter *spp-9p*::GFP fluorescence.

whether *dpy* gene products affect the DBL-1 ligand. Second, we used a transcriptional reporter for DBL-1 pathway activity, GFP expressed from the *spp-9* promoter (*spp-9p::gfp*). *spp-9* is a negatively regulated transcriptional target of the DBL-1 pathway that encodes a saposin-like protein, an innate immune response factor (Roberts *et al.*, 2010).

We tested these two reporters against *dpy* genes that encode structural components of the extracellular matrix. RNA interference (RNAi) of these genes in the GFP::DBL-1 background suggested that many affect DBL-1 ligand (Supplemental Table S3). We crossed these reporter transgenes into the panel of *dpy* mutants and examined their effect on reporter expression in 24-h adult hermaphrodites. Interestingly, all tested ECM mutants that significantly reduced GFP::DBL-1 fluorescence levels also affected *spp-9p::gfp* expression (Table 2B). This result confirms *spp-9p::gfp* reporter activity is strongly linked to the DBL-1 pathway.

Some extracellular matrix–associated genes had no effect on either GFP::DBL-1 or *spp-9p::gfp* expression: *dpy-1*/mucin and *dpy-2*, *dpy-7*, *dpy-8*, *dpy-9*, and *sqt-3/dpy-15* (Figure 1 and Table 2B). These results are consistent with these gene products having no effect on DBL-1 signaling. *dpy-3*, *dpy-5*, *dpy-6*, *dpy-10*, and *dpy-14* decreased GFP::DBL-1 fluorescence and increased *spp-9p::gfp* expression, consistent with loss of these gene products having a negative impact on DBL-1 signaling, suggesting feedback. Interestingly, other specific collagens that are DBL-1–regulated also show this feedback on DBL-1 signaling (Madaan *et al.*, 2019).

Notably, we discovered that *dpy-4*, *dpy-13*, and *dpy-17* significantly up-regulate *spp-9p::gfp* expression without affecting GFP::DBL-1 fluorescence (Figure 1; Table 2B). *C. elegans* DPY-17 is predicted to act downstream of DBL-1 secretion (Fotopoulos *et al.*, 2015). In other systems, basement membrane collagens bind BMPs and enhance their interaction with receptors, promoting downstream signaling (Paralkar *et al.*, 1990, 1992; Wang *et al.*, 2008). However, DPY-4, DPY-13, and DPY-17 are predicted cuticle collagens and therefore probably do not act between the secreting and receiving cells (see Figure 3 later in the paper). It is possible that these collagens indirectly regulate DBL-1 signaling targets by affecting the cuticle. Also, while loss of some collagen genes, including *dpy-2* and *dpy-7*, induced a robust stress response in *C. elegans*, loss of *dpy-4* and *dpy-13* failed to do so (Dodd *et al.*, 2018). The significant increase of *spp-9p::gfp* expression in *dpy-4* and *dpy-13*, but not in *dpy-2* or *dpy-7*, also supports the conclusion that *spp-9p::gfp* is

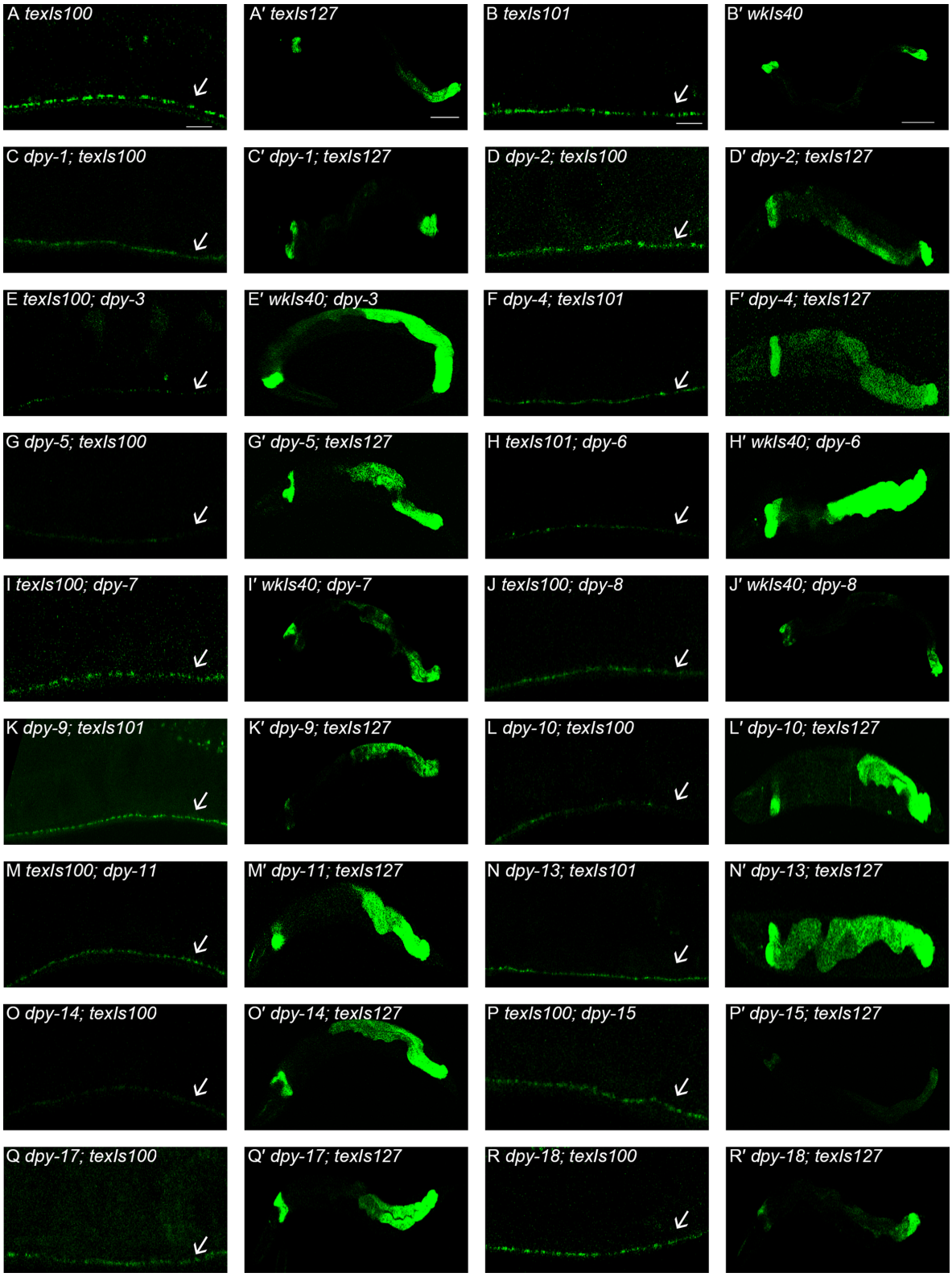

FIGURE 1: Effects of ECM-associated gene mutations on GFP::DBL-1 and DBL-1 pathway reporter *spp-9p*::GFP fluorescence. Arrows point to GFP::DBL-1 fluorescent punctae in A–R. Representative images show adult hermaphrodite expression of GFP::DBL-1 (A–R) and *spp- 9p*::GFP (A′–R′) in the following mutant backgrounds: A and B, wild type; C, *dpy-1*; D, *dpy-2*; E, *dpy-3*; F, *dpy-4*; G, *dpy-5*; H, *dpy-6*; I, *dpy-7*; J, *dpy-8*; K, *dpy-9*; L, *dpy-10*; M, *dpy-11*; N, *dpy-13*; O, *dpy-14*; P, *sqt-3/dpy-15*; Q, *dpy-17*; R, *dpy-18*; *dpy* mutants that reduced GFP-tagged DBL-1 and increased *spp-9p*::GFP activity are shown in E, G, H, L, and O. *dpy* mutants that increased *spp-9p*::GFP reporter activity without affecting GFP-tagged DBL-1 are shown in F, M, N, and Q. *dpy* mutants that had no effect on either of the reporters are shown in C, D, I, J, K, P, and R. Bars in A and B represent 10 and 100 µm, respectively.

strongly responsive to DBL-1 signaling and not to stress by cuticle alteration. Nonetheless, we show specificity of collagen regulation of DBL-1 signaling, because some known cuticle collagens have no effect on DBL-1 signaling in one-day adults (DPY-2, DPY-7, DPY-9, and SQT-3/DPY-15). It should be noted, though, that some collagens are known to be expressed at certain stages in *C. elegans*, so some ECM-associated *dpy* genes may affect DBL-1 signaling at other stages, which we would not have identified in this study (Celniker *et al.*, 2009; Jackson *et al.*, 2014; Madaan *et al.*, 2019).

In addition, we tested these two reporters against two *dpy* genes that encode ECM-processing enzymes. DPY-18 is a prolyl-4-hydroxylase alpha catalytic subunit, which in other organisms is required for collagen secretion as well as triple-helix assembly and stability (Mazzorana *et al.*, 1993; Brodsky and Ramshaw, 1997; Walmsley *et al.*, 1999; Hill *et al.*, 2000). *dpy-11* encodes a hypodermally expressed disulfide oxidoreductase that is predicted to modify extracellular matrix constituents (Nishiwaki and Miwa, 1998; Ko and Chow, 2002). Based on their phenotypes, both of these gene products may affect both cuticle and basement membrane (Nishiwaki and Miwa, 1998; Hill *et al.*, 2000; Ko and Chow, 2002; Torpe and Pocock, 2014). *dpy-18* loss had no effect on either DBL-1 pathway reporter, but *dpy-11* loss affected *spp-9p*::GFP without affecting the ligand within the secreting cell (Figure 1; Table 2B).

Together, these results suggest that the DBL-1 pathway and *spp-9* target gene expression are sensitive to cuticle-related factors that indirectly impact DBL-1 signaling.

Other body size genes interact genetically with the DBL-1 pathway

dpy-19 encodes a C-mannosyltransferase (Buettner *et al.*, 2013). *dpy-19(e1259)* resulted in significantly higher *spp-9p::gfp* reporter activity but did not alter GFP-tagged DBL-1 fluorescence levels (Figure 2; Table 2C). This enzyme family recognizes W-x-x-W motifs and adds α-mannose to the tryptophans in these motifs. *C. elegans* DBL-1 has a conserved W-x-x-W motif and may be a direct target of DPY-19. However, ADAMTS protease ADT-2/SMA-21 regulates DBL-1 signaling positively, and ADAMTS proteases are also targets of this enzyme family (Fernando *et al.*, 2011; Ihara *et al.*, 2015). ADT-2/SMA-21 isoforms have up to seven W-x-x-W or W-x-x-W-x-x-W motifs (Fernando *et al.*, 2011). Therefore, DPY-19 may regulate DBL-1 signaling directly through DBL-1's W-x-x-W motif, which may not affect DBL-1 localization within secreting cells but may affect DBL-1's ability to activate its receptors. Alternatively, DPY-19 may regulate DBL-1 signaling indirectly through modification of an ADAMTS protease.

Some sex and dosage compensation mutants are also shorter, perhaps from overexpression of X-linked body size genes (Meyer, 2005). We tested one of these, *dpy-21*, a dosage compensation–complex subunit (Yonker and Meyer, 2003). Loss of *dpy-21* increased DBL-1 pathway reporter expression but did not affect the GFP-tagged DBL-1 ligand (Figure 2; Table 2C).

dpy-23/apm-2 encodes the adaptor protein complex 2 (AP2) mu subunit. *dpy-23(e840)*, a 100-kb deletion that removes 18 open reading frames, significantly reduces GFP-tagged DBL-1 fluorescence and increases reporter activity (Figure 2; Table 2C; Gu *et al.*, 2008). DPY-23 is involved in protein trafficking, including the trafficking of the DBL-1 receptor SMA-6, which affects DBL-1 signaling (Gleason *et al.*, 2014). Feedback caused by loss of the DBL-1 receptor SMA-6 at the membrane could decrease ligand expression. However, DPY-23 is also expressed in the same neurons as DBL-1 and may play a direct role in the secretion of DBL-1 (Shim and Lee, 2000). While all phenotypes associated with *e840* deletion are fully rescued by expression of wild-type *dpy-23*, it is possible that the DBL-1–associated phenotypes identified here are caused by a different part of the *e840* deletion (Gu *et al.*, 2008).

Two putative transcription factor genes also were tested. Loss of the BED zinc-finger protein gene *dpy-20* had no effect on GFP-tagged DBL-1 fluorescence or *spp-9* transcriptional reporter expression (Figure 2; Table 2C). However, loss of the SET domain and the zinc-finger protein gene *blmp-1/dpy-24* significantly reduced GFP-tagged DBL-1 fluorescence and increased *spp-9* transcriptional reporter expression (Figure 2; Table 2C). This result supports a genetic interaction between BLMP-1 and the DBL-1 pathway. Another *C. elegans* superfamily member related to DBL-1, *daf-7*,

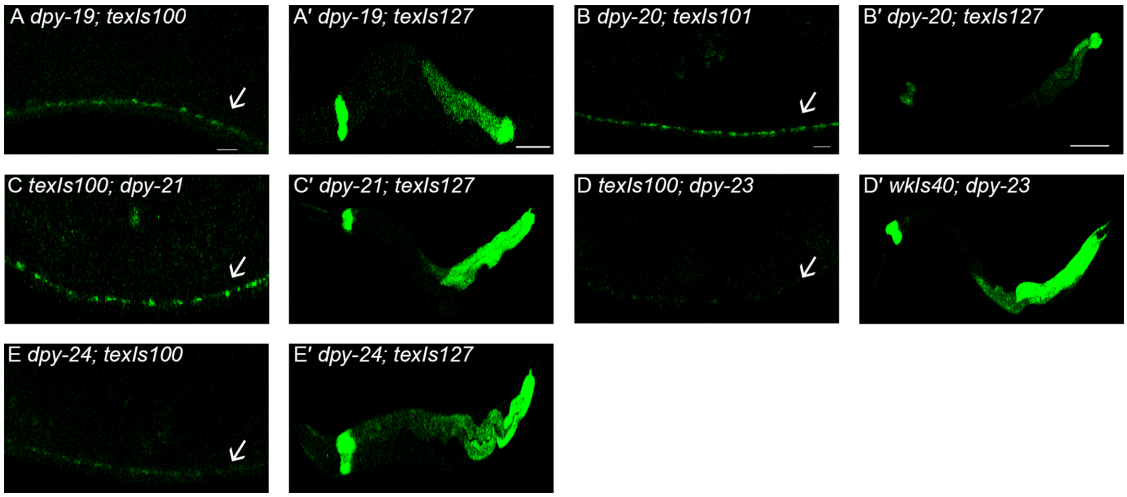

FIGURE 2: Effects of other body size–associated gene mutations on GFP::DBL-1 and DBL-1 pathway reporter *spp-9p*::GFP fluorescence. Arrows point to GFP::DBL-1 fluorescent punctae in A–E. Representative images show adult hermaphrodite expression of GFP::DBL-1 (A–E) and *spp-9p*::GFP (A′–E′) in the following mutant backgrounds: A, *dpy-19*; B, *dpy-20*; C, *dpy-21*; D, *dpy-23*; E, *dpy-24*. Compare to controls in Figure 1. *dpy* mutants that reduced GFP-tagged DBL-1 and increased *spp-9p*::GFP activity are shown in D and E. *dpy* mutants that increased *spp-9p*::GFP reporter activity without affecting GFP-tagged DBL-1 are shown in A and C. A *dpy* mutant that had no effect on either of the reporters is shown in B. Bars in A and B represent 10 and 100 μm, respectively.

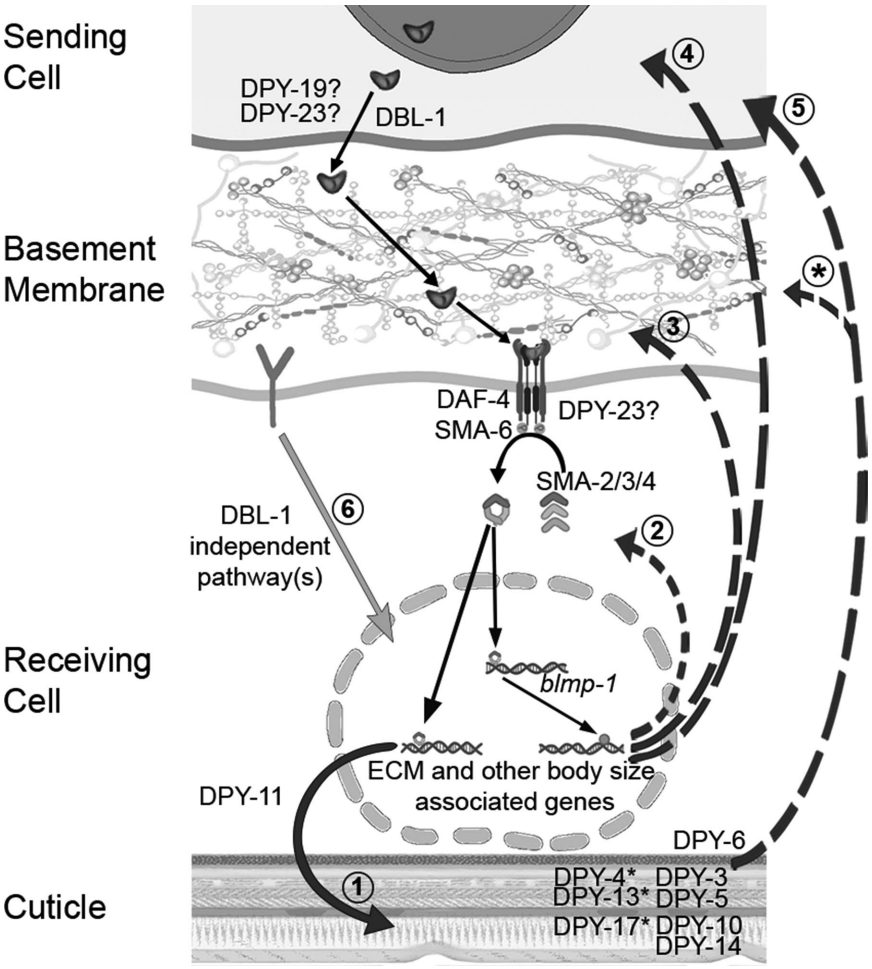

FIGURE 3: Proposed model of body size regulation by the DBL-1 pathway and *dpy* body size–associated genes in *C. elegans*. Within the sending cell, DBL-1 may be modified by DPY-19/C-mannosyltransferase and transported by the AP2 complex, which includes the DPY-23/AP2 mu subunit. Signaling through the receptor complex may also be controlled by DPY-23. DBL-1 signaling directly controls the expression of cuticle components, which affects body size (arrow 1). DPY-11/disulfide oxidoreductase may process DBL-1-regulated cuticle components before secretion. DBL-1–regulated gene expression, in part through BLMP-1, may modulate signaling within the receiving cell (arrow 2) or between the sending and receiving cells (arrow 3), or may feed back on the sending cell (arrow 4). Cues from the receiving cell or cuticle may be received (indirectly) by the sending cell and affect DBL-1 expression or secretion (arrow 5) or affect signaling downstream of DBL-1 secretion (starred arrowhead in arrow 5 and starred DPY collagens). Other cell-signaling pathways act independent of DBL-1 to control body size (arrow 6). Dashed lines represent potential indirect regulation. *dpy* gene products that had no effect on DBL-1 signaling are not included in this model.

requires *blmp-1* for proper signaling (Hyun *et al.*, 2016). In mammals, BLIMP1 is highly regulated by the TGF-β pathway (Salehi *et al.*, 2012; Telerman *et al.*, 2017).

Regulation of body size–associated genes by DBL-1

TGF-β pathways regulate ECM genes in many systems, both directly and indirectly (Morikawa *et al.*, 2011; Kim *et al.*, 2018; Madaan *et al.*, 2018). In *C. elegans*, microarray analyses showed that some ECM genes are highly regulated by this pathway (Mochii *et al.*, 1999; Liang *et al.*, 2003; Roberts *et al.*, 2010). Furthermore, ChIP-seq analyses showed that the DBL-1 pathway signal transducer SMA-3 binds the regulatory region of the cuticle collagen genes *col-141* and *col-142* (Madaan *et al.*, 2018). To better understand the interplay between the DBL-1 pathway and other body size players, we performed RNA-seq analyses on wild-type and *dbl-1(nk3)* strains. Like previous microarray results, we identified several cuticle-associated genes that were down-regulated in the *dbl-1(nk3)* strain as compared with the wild type (Supplemental Table S4). However, our panel of regulated genes is overlapping but more extensive. In addition, we identified SMA-3 binding sites upstream of body size–associated genes by interrogating the SMA-3 MODENCODE data set (Gerstein *et al.*, 2010). We also determined that *blmp-1* is highly regulated by DBL-1. Notably, SMA-3 binds within 1000 bp upstream of *blmp-1*, suggesting that *C. elegans* BLMP-1 is transcriptionally regulated by DBL-1/BMP, as seen by TGF-β regulation of BLIMP1 in other systems (Gerstein *et al.*, 2010; Salehi *et al.*, 2012; Telerman *et al.*, 2017). BLMP-1 binds upstream of most of the ECM-associated genes that are differentially regulated by DBL-1, suggesting that DBL-1 signaling regulates these ECM genes through transcriptional control of BLMP-1 (Supplemental Table S4) (Gerstein *et al.*, 2010). It remains to be experimentally determined whether this correlation is physiologically relevant.

Concluding remarks

In this work, we have presented the analysis of a *lon-2(-)* suppressor screen and a related panel of body size–associated *dpy* genes. We have identified complex interactions between DBL-1 signaling and other body size regulators, which have previously been presumed to act independent of DBL-1 signaling. This work supports the model that the DBL-1 pathway is a master regulator of several processes that together affect the body size trait, and some body size–associated genes also feed back on the DBL-1 pathway (Figure 3; Mochii *et al.*, 1999; Roberts *et al.*, 2010; Liang *et al.*, 2013; Madaan *et al.*, 2018, 2019). Some DBL-1 pathway suppressors and other body size–associated genes may be regulated directly by the DBL-1 pathway Smads. However, expression of other body size–associated genes may be controlled by DBL-1–regulated transcription factors such as BLMP-1/DPY-24. We are poised to define the molecular and cellular relevance of the genetic interactions between DBL-1 signaling and other body size regulators, including the uncloned loci, DPY-6/mucin-like protein, intraflagellar transport proteins, DPY-19/C-mannosyltransferase, and BLMP-1/DPY-24/transcription regulator.

MATERIALS AND METHODS

Strains and maintenance

C. elegans strains used in these studies were derived from the wild-type variety Bristol strain N2 and were cultured on modified EZ nematode growth media plates as previously described (Madhu *et al.*, 2019). All strains were cultured on *Escherichia coli* strain OP50

at 20°C. Strains generated and used are listed in Supplemental Table S1. Double mutant lines were generated using standard genetic crosses.

The transgenic alleles *texIs100 [dbl-1::dbl-1:gfp; ttx-3p::rfp]* IV and *texIs101 [dbl-1::dbl-1:gfp; ttx-3p::rfp]* V were created by UV/TMP mutagenesis of an extrachromosomal array (Beifuss and Gumienny, 2012). *wkEx52* (*spp-9p::gfp*) was integrated using an established UV/TMP mutagenesis procedure to yield *texIs127* X (Yandell *et al.*, 1994). These integrated transgenes were backcrossed five times and mapped. *wkEx52(spp-9p::gfp)* was integrated into N2 animals using an x-ray source to yield *wkIs40*. This strain was backcrossed four times to the N2 wild-type strain. The resulting strain was named LT998.

Double mutants with *texIs100*, *texIs101*, *texIs127*, and *wkIs40,* and the triple mutant strain TLG281 *rrf-3*(*pk1426*) II; *texIs100* IV; *dbl-1*(*nk3*) V were constructed by standard methods (Supplemental Table S1) (Brenner, 1974). A complete list of strains used in this work is provided in Table 1 and Supplemental Table S1.

Forward genetic screen for suppressors of the *lon-2(e678)* long phenotype

To identify factors involved in regulating DBL-1 pathway-mediated body length, *lon-2(e678)* hermaphrodites were mutagenized with 50 mM ethyl methanesulfonate (EMS) as previously described (Brenner, 1974; Savage-Dunn *et al.*, 2003). Mutagenized animals were transferred to plates to self-propagate. F1 animals were transferred two to a plate to self. F2 populations were scored for a reduced body length in about one-eighth of the population, assuming a recessive mutation. Only one animal from each plate containing a candidate mutant was maintained, to confirm that each candidate was independently obtained. About 9000 mutagenized genomes were scored (less than saturation), and lines with high body size–phenotype penetrance and expressivity, and with good health, were selected for characterization. Animals that showed other phenotypes, including rolling movement (Rol) and reduced viability or sterility, were excluded. Mutants were outcrossed five times to N2 before further analyses. Outcrossing also identified whether alleles resided on the X chromosome or an autosome. Mutations were complementation-tested for allelism with known DBL-1 pathway genes. Alleles of novel loci were then tested for linkage to STS markers or to *unc-15(e73)* I, *unc-104(e1265)* II, *unc-32(e189)* III, *unc-5(e53)* IV, and *unc-23(e25)* V (Williams *et al.*, 1992). Next, mutations mapping to the same linkage group were complementation-tested to each other and candidate gene mutant alleles. Some alleles were further mapped using standard two-factor, three-factor, and SNP mapping techniques (Brenner, 1974; Wicks *et al.*, 2001).

RNA interference

RNAi by bacterial feeding was performed as previously described (Timmons and Fire, 1998). The *C. elegans* strain TLG281 *rrf-3*(*pk1426*) II; *texIs100* IV; *dbl-1*(*nk3*) V was used for this experiment (Beifuss and Gumienny, 2012). Bacteria from the Vidal and Ahringer cDNA libraries (Open Biosystems and Source BioScience, respectively) were used (Kamath and Ahringer, 2003; Rual *et al.*, 2004). C06C3.5, a predicted pseudogene, was used as the negative control. *bli-4(RNAi)* was used as the positive control (Thacker *et al.*, 1995). Bacteria from single colonies were grown overnight in Luria–Bertani broth (Sigma, St. Louis, MO) containing 50 µg/ml carbenicillin (Gold Biotechnology, St. Louis, MO) and induced to express dsRNA using 1 µg/ml isopropyl β-D-1-thiogalactopyranoside (IPTG) for 4 h. After induction, bacterial broth was plated on nematode growth medium containing 50 µg/ml carbenicillin and 1 µg/ml IPTG and dried. Embryos staged by bleaching were transferred to these plates and grown to the young adult stage for observation as previously described (Kamath and Ahringer, 2003; Rual *et al.*, 2004; Beifuss and Gumienny, 2012).

Imaging

C. elegans adults 24 h post-L4 were anesthetized using 1 mM levamisole hydrochloride (Sigma, St. Louis, MO) for fluorescence and body size imaging.

Fluorescence imaging. Fluorescence imaging for RNAi and mutant studies was performed using a Nikon A1 confocal system (Nikon Instruments, Melville, NY). A 60× objective was used to capture GFP::DBL-1 intensities. Fluorescence intensities of *spp-9p::gfp* were captured using a 10× objective. Microscope settings were standardized to obtain fluorescence intensity values in the measurable dynamic range for both control and experimental samples, and these image-capture conditions were kept constant throughout the experiments. Mean fluorescence intensities were measured using Nikon NIS Elements AR-5.02 software.

Body size imaging. For RNAi studies, animals were imaged using the same confocal system with a 10× objective to measure their body length. Body size was quantified using NIS Elements AR-5.02 imaging software.

For mutant studies, animals were imaged to measure body size using a Nikon SMZ1500 dissecting microscope (Nikon, Melville, NY). Body size was measured using the length measurement image tool within iVision-Mac (BioVision Technologies, Exton, PA).

RNA-seq

We used two biological replicates of wild-type and *dbl-1(nk3)* populations for RNA sequencing with the Illumina MiSeq system. Animals were staged by bleaching and harvested for RNA extraction at the 48 h post-L4 stage. RNA extraction was performed using the freeze-cracking method as previously described (Portman, 2006). A total of 2 µg of total RNA of each sample was used for TruSeq Stranded mRNA sample preparation using the low sample protocol per manufacturer's instructions (Illumina). RNA and cDNA concentrations were measured by a Qubit fluorometer (Molecular Probes, Life Technologies). The quality of RNA and cDNA was assessed by an Experion automated electrophoresis system (BioRad). The libraries were sequenced with ~40–50 million total reads and FASTQ quality scores of the raw data from sequencing were generated. The reads were mapped against the *C. elegans* genome ce10 (UCSC RefSeq gene annotation) using the STAR aligner (RNA-Seq Alignment, Illumina). On the average, 97.9% of reads were aligned. Cufflinks 2 was used for the FPKM estimation of reference genes and transcripts. Differential gene expression analysis was performed with Cuffdiff2 using the Cufflinks Assembly and DE application (Illumina). Candidates with a *q* value <0.05 were classified as differentially expressed genes.

Statistical analysis

We used at least seven animals to quantify GFP::DBL-1 fluorescence and at least 10 animals to measure body size for RNAi studies. For the mutant studies, we used at least 10 animals to quantify GFP::DBL-1 fluorescence intensities and at least 15 animals to measure *spp-9p::gfp* fluorescence intensities. We used at least 30 animals to determine body size for the mutant studies. Mean fluorescence intensities and body length values of test populations were calculated as percentages of their respective controls with 95% confidence intervals. Statistical analyses were performed

using an independent *t* test to compare test and control sample means.

Data and reagent availability

Strains listed in Table 1 and Supplemental Table S1 are available upon request.

ACKNOWLEDGMENTS

We thank Lisa Maduzia, Huang Wang, Adam Auerbach, James Cignarella, Lena Chin, Steven Cohen, and Archna Sinha for mutant screening. We thank Bryce Chiang, Naomi Klassel, Andrew Roberts, Tara Wahab, Shi-Lan Wu, and Cole Zimmerman for complementation testing and/or mapping. Aileen Salazar created some double mutant strains. Stefan Eimer provided *dpy-1* cloning information. We thank Cathy Savage-Dunn and members of the Padgett lab, including Luke Huggins and Pradeep Das, and the Gumienny lab, including Geethanjali Ravindranathan, Sanil Sansar, and Neethu Issac, for constructive discussion. Sujata Agarwal designed the Figure 3 model. Pamela Padilla provided some RNAi constructs. Some strains were obtained from the *Caenorhabditis* Genetics Center (CGC), which is funded by the NIH Office of Research Infrastructure Programs (P40 OD010440). We thank WormBase. This work was supported by National Institutes of Health grants F32 GM066445, T32-MH/AG19957-06A2, and R01 GM097591, a Charles and Johanna Busch Postdoctoral Fellowship, and a TWU Chancellor's Research Fellowship to T.L.G., and internal funding by Texas Woman's University. This work is dedicated to family and friends.

REFERENCES

Aravind L (2000). The BED finger, a novel DNA-binding domain in chromatin-boundary-element-binding proteins and transposases. Trends Biochem Sci 25, 421–423.

Bacaj T, Lu Y, Shaham S (2008). The conserved proteins CHE-12 and DYF-11 are required for sensory cilium function in *Caenorhabditis elegans*. Genetics 178, 989–1002.

Baird SE, Emmons SW (1990). Properties of a class of genes required for ray morphogenesis in *Caenorhabditis elegans*. Genetics 126, 335–344.

Beifuss KK, Gumienny TL (2012). RNAi screening to identify postembryonic phenotypes in *C. elegans*. J Vis Exp 2012, e3442.

Brenner S (1974). The genetics of *Caenorhabditis elegans*. Genetics 77, 71–94.

Brodsky B, Ramshaw JA (1997). The collagen triple-helix structure. Matrix Biol 15, 545–554.

Buettner FF, Ashikov A, Tiemann B, Lehle L, Bakker H (2013). *C. elegans* DPY-19 is a C-mannosyltransferase glycosylating thrombospondin repeats. Mol Cell 50, 295–302.

Celniker SE, Dillon LA, Gerstein MB, Gunsalus KC, Henikoff S, Karpen GH, Kellis M, Lai EC, Lieb JD, MacAlpine DM, *et al.* (2009). Unlocking the secrets of the genome. Nature 459, 927–930.

Clark DV, Suleman DS, Beckenbach KA, Gilchrist EJ, Baillie DL (1995). Molecular cloning and characterization of the *dpy-20* gene of *Caenorhabditis elegans*. Mol Gen Genet 247, 367–378.

Dodd W, Tang L, Lone JC, Wimberly K, Wu CW, Consalvo C, Wright JE, Pujol N, Choe KP (2018). A damage sensor associated with the cuticle coordinates three core environmental stress responses in *Caenorhabditis elegans*. Genetics 208, 1467–1482.

Fernando T, Flibotte S, Xiong S, Yin J, Yzeiraj E, Moerman DG, Meléndez A, Savage-Dunn C (2011). *C. elegans* ADAMTS ADT-2 regulates body size by modulating TGFβ signaling and cuticle collagen organization. Dev Biol 352, 92–103.

Fotopoulos P, Kim J, Hyun M, Qamari W, Lee I, You YJ (2015). DPY-17 and MUA-3 interact for connective tissue-like tissue integrity in *Caenorhabditis elegans*: a model for Marfan syndrome. G3 (Bethesda) 5, 1371–1378.

Gerstein MB, Lu ZJ, Van Nostrand EL, Cheng C, Arshinoff BI, Liu T, Yip KY, Robilotto R, Rechtsteiner A, Ikegama K, *et al.* (2010). Integrative analysis of the *Caenorhabditis elegans* genome by the modENCODE project. Science 330, 1775–1787.

Gleason RJ, Akintobi AM, Grant BD, Padgett RW (2014). BMP signaling requires retromer-dependent recycling of the type I receptor. Proc Natl Acad Sci USA 111, 2578–2583.

Gleason RJ, Vora M, Li Y, Kane NS, Liao K, Padgett RW (2017). *C. elegans* SMA-10 regulates BMP receptor trafficking. PLoS One 12, e0180681.

Grover P, Nath S, Nye MD, Zhou R, Ahmad M, Mukherjee P (2018). SMAD4-independent activation of TGF-β signaling by MUC1 in a human pancreatic cancer cell line. Oncotarget 9, 6897–6910.

Gu M, Schuske K, Watanabe S, Liu Q, Baum P, Garriga G, Jorgensen EM (2008). Mu2 adaptin facilitates but is not essential for synaptic vesicle recycling in *Caenorhabditis elegans*. J Cell Biol 183, 881–892.

Gumienny TL, Macneil L, Zimmerman CM, Wang H, Chin L, Wrana JL, Padgett RW (2010). *Caenorhabditis elegans* SMA-10/LRIG is a conserved transmembrane protein that enhances bone morphogenetic protein signaling. PLoS Genet, e1000963.

Gumienny TL, MacNeil LT, Wang H, de Bono M, Wrana JL, Padgett RW (2007). Glypican LON-2 is a conserved negative regulator of BMP-like signaling in *Caenorhabditis elegans*. Curr Biol 17, 159–164.

Hill KL, Harfe BD, Dobbins CA, L'Hernault SW (2000). *dpy-18* encodes an alpha-subunit of prolyl-4-hydroxylase in *Caenorhabditis elegans*. Genetics 155, 1139–1148.

Hodgkin J (1983). Male phenotypes and mating efficiency in *Caenorhabditis elegans*. Genetics 103, 43–64.

Hyun M, Kim J, Dumur C, Schroeder FC, You YJ (2016). BLIMP-1/BLMP-1 and metastasis-associated protein regulate stress resistant development in *Caenorhabditis elegans*. Genetics 203, 1721–1732.

Ihara Y, Inai Y, Ikezaki M, Matsui ISL, Manabe S, Ito Y (2015). C-mannosylation: modification on tryptophan in cellular proteins. In: Glycoscience: Biology and Medicine, ed. N Taniguchi, T Endo, G Hart, P Seeberger, and CH Wong, Tokyo: Springer, 1091–1099.

Jackson BM, Abete-Luzi P, Krause MW, Eisenmann DM (2014). Use of an activated beta-catenin to identify Wnt pathway target genes in *Caenorhabditis elegans*, including a subset of collagen genes expressed in late larval development. G3 (Bethesda) 4, 733–747.

Jonckheere N, Perrais M, Mariette C, Batra SK, Aubert JP, Pigny P, Van Seuningen I (2004a). A role for human MUC4 mucin gene, the ErbB2 ligand, as a target of TGF-β in pancreatic carcinogenesis. Oncogene 23, 5729–5738.

Jonckheere N, Van Der Sluis M, Velghe A, Buisine MP, Sutmuller M, Ducourouble MP, Pigny P, Büller HA, Aubert JP, Einerhand AW, Van Seuningen I (2004b). Transcriptional activation of the murine Muc5ac mucin gene in epithelial cancer cells by TGF-β/Smad4 signalling pathway is potentiated by Sp1. Biochem J 377, 797–808.

Kamath RS, Ahringer J (2003). Genome-wide RNAi screening in *Caenorhabditis elegans*. Methods 30, 313–321.

Kim KK, Sheppard D, Chapman HA (2018). TGF-β1 signaling and tissue fibrosis. Cold Spring Harb Perspect Biol 10, a022293.

Ko FC, Chow KL (2002). A novel thioredoxin-like protein encoded by the *C. elegans dpy-11* gene is required for body and sensory organ morphogenesis. Development 129, 1185–1194.

Kobayashi T, Gengyo-Ando K, Ishihara T, Katsura I, Mitani S (2007). IFT-81 and IFT-74 are required for intraflagellar transport in *C. elegans*. Genes Cells 12, 593–602.

Krishna S, Maduzia LL, Padgett RW (1999). Specificity of TGFβ signaling is conferred by distinct type I receptors and their associated SMAD proteins in *Caenorhabditis elegans*. Development 126, 251–260.

Li Q, Liu G, Shao D, Wang J, Yuan H, Chen T, Zhai R, Ni W, Tai G (2015a). Mucin1 mediates autocrine transforming growth factor β signaling through activating the c-Jun N-terminal kinase/activator protein 1 pathway in human hepatocellular carcinoma cells. Int J Biochem Cell Biol 59, 116–125.

Li Q, Liu G, Yuan H, Wang J, Guo Y, Chen T, Zhai R, Ni W, Tai G (2015b). Mucin1 shifts Smad3 signaling from the tumor-suppressive pSmad3C/p21(WAF1) pathway to the oncogenic pSmad3L/c-Myc pathway by activating JNK in human hepatocellular carcinoma cells. Oncotarget 6, 4253–4265.

Liang J, Lints R, Foehr ML, Tokarz R, Yu L, Emmons SW, Liu J, Savage-Dunn C (2003). The *Caenorhabditis elegans* schnurri homolog *sma-9* mediates stage- and cell type-specific responses to DBL-1 BMP-related signaling. Development 130, 6453–6464.

Liang J, Xiong S, Savage-Dunn C (2013). Using RNA-mediated interference feeding strategy to screen for genes involved in body size regulation in the nematode *C. elegans*. J Vis Exp 2013, 4373.

Liang J, Yu L, Yin J, Savage-Dunn C (2007). Transcriptional repressor and activator activities of SMA-9 contribute differentially to BMP-related signaling outputs. Dev Biol 305, 714–725.

Luo S, Shaw WM, Ashraf J, Murphy CT (2009). TGF-β Sma/Mab signaling mutations uncouple reproductive aging from somatic aging. PLoS Genet 5, e1000789.
Madaan U, Faure L, Chowdhury A, Ahmed S, Ciccarelli EJ, Gumienny TL, Savage-Dunn C (2019). Feedback regulation of BMP signaling by *C. elegans* cuticle collagens. bioRxiv 686592.
Madaan U, Yzeiraj E, Meade M, Clark JF, Rushlow CA, Savage-Dunn C (2018). BMP signaling determines body size via transcriptional regulation of collagen genes in *Caenorhabditis elegans*. Genetics 210, 1355–1367.
Madhu B, Salazar AE, Gumienny TL (2019). *Caenorhabditis elegans* egg-laying and brood-size changes upon exposure to *Serratia marcescens* and *Staphylococcus epidermidis* are independent of DBL-1 signaling. microPublication Biology, 10.17912/2r51-b476.
Maduzia LL, Roberts AF, Wang H, Lin X, Chin LJ, Zimmerman CM, Cohen S, Feng XH, Padgett RW (2005). *C. elegans* serine-threonine kinase KIN-29 modulates TGFβ signaling and regulates body size formation. BMC Dev Biol 5, 8.
Mazzorana M, Gruffat H, Sergeant A, van der Rest M (1993). Mechanisms of collagen trimer formation. Construction and expression of a recombinant minigene in HeLa cells reveals a direct effect of prolyl hydroxylation on chain assembly of type XII collagen. J Biol Chem 268, 3029–3032.
Meyer BJ (2005). X-chromosome dosage compensation. In: WormBook, ed. The *C. elegans* Research Community, doi/10.1895/wormbook.1.8.1.
Mochii M, Yoshida S, Morita K, Kohara Y, Ueno N (1999). Identification of transforming growth factor-β- regulated genes in *Caenorhabditis elegans* by differential hybridization of arrayed cDNAs. Proc Natl Acad Sci USA 96, 15020–15025.
Morikawa M, Koinuma D, Tsutsumi S, Vasilaki E, Kanki Y, Heldin CH, Aburatani H, Miyazono K (2011). ChIP-seq reveals cell type-specific binding patterns of BMP-specific Smads and a novel binding motif. Nucleic Acids Res 39, 8712–8727.
Morita K, Chow KL, Ueno N (1999). Regulation of body length and male tail ray pattern formation of *Caenorhabditis elegans* by a member of TGF-β family. Development 126, 1337–1347.
Nishiwaki K, Miwa J (1998). Mutations in genes encoding extracellular matrix proteins suppress the *emb-5* gastrulation defect in *Caenorhabditis elegans*. Mol Gen Genet 259, 2–12.
Nystrom J, Shen ZZ, Aili M, Flemming AJ, Leroi A, Tuck S (2002). Increased or decreased levels of *Caenorhabditis elegans lon-3*, a gene encoding a collagen, cause reciprocal changes in body length. Genetics 161, 83–97.
Page AP, Johnstone IL (2007). The cuticle. In: WormBook, ed. The *C. elegans* Research Community, doi/10.1895/wormbook.1.138.1.
Paralkar VM, Nandedkar AK, Pointer RH, Kleinman HK, Reddi AH (1990). Interaction of osteogenin, a heparin binding bone morphogenetic protein, with type IV collagen. J Biol Chem 265, 17281–17284.
Paralkar VM, Weeks BS, Yu YM, Kleinman HK, Reddi AH (1992). Recombinant human bone morphogenetic protein 2B stimulates PC12 cell differentiation: potentiation and binding to type IV collagen. J Cell Biol 119, 1721–1728.
Portman DS (2006). Profiling *C. elegans* gene expression with DNA microarrays. WormBook, 1–11.
Roberts AF, Gumienny TL, Gleason RJ, Wang H, Padgett RW (2010). Regulation of genes affecting body size and innate immunity by the DBL-1/BMP-like pathway in *Caenorhabditis elegans*. BMC Dev Biol 10, 61.
Rual JF, Ceron J, Koreth J, Hao T, Nicot AS, Hirozane-Kishikawa T, Vandenhaute J, Orkin SH, Hill DE, van den Heuvel S, *et al.* (2004). Toward improving *Caenorhabditis elegans* phenome mapping with an ORFeome-based RNAi library. Genome Res 14, 2162–2168.
Salehi S, Bankoti R, Benevides L, Willen J, Couse M, Silva JS, Dhall D, Meffre E, Targan S, Martins GA (2012). Blimp-1 contributes to intestinal mucosa homeostasis by limiting the number of IL-17-producing CD4+ T cells. J Immunol 189, 5682–5693.
Savage C, Das P, Finelli AL, Townsend SR, Sun CY, Baird SE, Padgett RW (1996). *Caenorhabditis elegans* genes *sma-2*, *sma-3*, and *sma-4* define a conserved family of transforming growth factor β pathway components. Proc Natl Acad Sci USA 93, 790–794.
Savage-Dunn C, Maduzia LL, Zimmerman CM, Roberts AF, Cohen S, Tokarz R, Padgett RW (2003). Genetic screen for small body size mutants in *C. elegans* reveals many TGFβ pathway components. Genesis 35, 239–247.
Schertel C, Conradt B (2007). *C. elegans* orthologs of components of the RB tumor suppressor complex have distinct pro-apoptotic functions. Development 134, 3691–3701.
Schultz RD, Bennett EE, Ellis EA, Gumienny TL (2014). Regulation of extracellular matrix organization by BMP signaling in *Caenorhabditis elegans*. PLoS One 9, e101929.
Shen X, Valencia CA, Gao W, Cotten SW, Dong B, Huang BC, Liu R (2008). Ca^{2+}/Calmodulin-binding proteins from the *C. elegans* proteome. Cell Calcium 43, 444–456.
Shim J, Lee J (2000). Molecular genetic analysis of *apm-2* and *aps-2*, genes encoding the medium and small chains of the AP-2 clathrin-associated protein complex in the nematode *Caenorhabditis elegans*. Mol Cells 10, 309–316.
Starich TA, Herman RK, Kari CK, Yeh WH, Schackwitz WS, Schuyler MW, Collet J, Thomas JH, Riddle DL (1995). Mutations affecting the chemosensory neurons of *Caenorhabditis elegans*. Genetics 139, 171–188.
Suzuki Y, Yandell MD, Roy PJ, Krishna S, Savage-Dunn C, Ross RM, Padgett RW, Wood WB (1999). A BMP homolog acts as a dose-dependent regulator of body size and male tail patterning in *Caenorhabditis elegans*. Development 126, 241–250.
Telerman SB, Rognoni E, Sequeira I, Pisco AO, Lichtenberger BM, Culley OJ, Viswanathan P, Driskell RR, Watt FM (2017). Dermal Blimp1 acts downstream of epidermal TGFβ and Wnt/beta-catenin to regulate hair follicle formation and growth. J Invest Dermatol 137, 2270–2281.
Thacker C, Peters K, Srayko M, Rose AM (1995). The *bli-4* locus of *Caenorhabditis elegans* encodes structurally distinct kex2/subtilisin-like endoproteases essential for early development and adult morphology. Genes Dev 9, 956–971.
Timmons L, Fire A (1998). Specific interference by ingested dsRNA. Nature 395, 854.
Torpe N, Pocock R (2014). Regulation of axonal midline guidance by prolyl 4-hydroxylation in *Caenorhabditis elegans*. J Neurosci 34, 16348–16357.
Walmsley AR, Batten MR, Lad U, Bulleid NJ (1999). Intracellular retention of procollagen within the endoplasmic reticulum is mediated by prolyl 4-hydroxylase. J Biol Chem 274, 14884–14892.
Wang X, Harris RE, Bayston LJ, Ashe HL (2008). Type IV collagens regulate BMP signalling in *Drosophila*. Nature 455, 72–77.
Wicks SR, Yeh RT, Gish WR, Waterston RH, Plasterk RH (2001). Rapid gene mapping in *Caenorhabditis elegans* using a high density polymorphism map. Nat Genet 28, 160–164.
Williams BD, Schrank B, Huynh C, Shownkeen R, Waterston RH (1992). A genetic mapping system in *Caenorhabditis elegans* based on polymorphic sequence-tagged sites. Genetics 131, 609–624.
Yandell MD, Edgar LG, Wood WB (1994). Trimethylpsoralen induces small deletion mutations in *Caenorhabditis elegans*. Proc Natl Acad Sci USA 91, 1381–1385.
Yemini E, Jucikas T, Grundy LJ, Brown AE, Schafer WR (2013). A database of *Caenorhabditis elegans* behavioral phenotypes. Nat Methods 10, 877–879.
Yonker SA, Meyer BJ (2003). Recruitment of *C. elegans* dosage compensation proteins for gene-specific versus chromosome-wide repression. Development 130, 6519–6532.